diffraction. The work was supported by NSF Grant CHE 76-83665. Spectra were recorded in Ames Laboratory, U.S. Department of Energy.

Registry No. $Mo_2(O_2CCH_3)_4$, 14221-06-8.

References and Notes

(1) C. D. Cowman and H. B. Gray, *J. Am. Chem. Soc.*, **95**, 8177 (1973).
(2) A. P. Mortola, J. W. Moskowitz, N. Rosch, C. D. Cowman, and H. B. Gray, *Chem. Phys. Lett.*, **32**, 283 (1975).
(3) F. A. Cotton, B. A. Frenz, B. R. Stults, and T. R. Webb, *J. Am. Chem. Soc.*, **98**, 2768 (1976).
(4) P. E. Fanwick, D. S. Martin, F. A. Cotton, and T. R. Webb, *Inorg. Chem.*, **16**, 2103 (1977).
(5) J. G. Norman and H. J. Kolari, *J. Am. Chem. Soc.*, **97**, 33 (1975).
(6) F. A. Cotton, D. S. Martin, P. E. Fanwick, T. J. Peters, and T. R. Webb, *J. Am. Chem. Soc.*, **98**, 4681 (1976).
(7) P. E. Fanwick, D. S. Martin, Jr., T. R. Webb, G. A. Robbins, and R. A. Newman, *Inorg. Chem.*, **17**, 2723 (1978).
(8) F. A. Cotton, D. S. Martin, T. R. Webb, and T. J. Peters, *Inorg. Chem.*, **15**, 1199 (1976).
(9) W. C. Trogler, E. I. Solomon, Ib Trajberg, C. J. Ballhausen, and H. B. Gray, *Inorg. Chem.*, **16**, 828 (1977).
(10) F. A. Cotton, Z. C. Mester, and T. R. Webb, *Acta Crystallogr., Sect. B*, **30**, 2768 (1974).
(11) D. S. Martin, Jr., *Inorg. Chim. Acta Rev.*, **5**, 107 (1971).
(12) S. Pancharatnam, *Proc. Indian Acad. Sci., Sect. A*, **42**, 86 (1955).
(13) R. F. Stewart and N. Davidson, *J. Chem. Phys.*, **39**, 255 (1963).
(14) W. K. Bratton, F. A. Cotton, and M. DeBeau, *J. Coord. Chem.*, **1**, 121 (1971).
(15) D. P. Craig and G. J. Small, *J. Chem. Phys.*, **50**, 3827 (1969).
(16) E. Hutchisson, *Phys. Rev.*, **39**, 410 (1930); **37**, 45 (1931).
(17) E. S. Yeung, *J. Mol. Spectrosc.*, **45**, 142 (1973).
(18) J. G. Norman, Jr., and H. J. Kolari, *J. Chem. Soc., Chem. Commun.*, 649 (1975).
(19) J. G. Norman, Jr., H. J. Kolari, H. B. Gray, and W. C. Trogler, *Inorg. Chem.*, **16**, 987 (1978).
(20) F. A. Cotton, P. E. Fanwick, L. D. Gage, B. Kalbacher, and D. S. Martin, Jr., *J. Am. Chem. Soc.*, **99**, 5642 (1977).
(21) F. A. Cotton, B. A. Frenz, E. Pedersen, and T. R. Webb, *Inorg. Chem.*, **14**, 391 (1975).
(22) D. P. Craig and S. H. Walmsley, "Excitons in Molecular Crystals", W. A. Benjamin, New York, N.Y., 1968, Chapter 6.

Contribution from the Structural Chemistry Group, Department of Chemistry, Indian Institute of Technology, Madras 600036, India, and Research School of Chemistry, The Australian National University, Canberra ACT 2600, Australia

Electron Paramagnetic Resonance Studies of Two Low-Spin Hexacoordinate Di(tertiary phosphine) Complexes of Nickel(III)

C. N. SETHULAKSHMI,[1a] S. SUBRAMAINAN,[1a] M. A. BENNETT,[1b] and P. T. MANOHARAN*[1a]

Received December 27, 1978

Single-crystal EPR studies on $[Ni(DP)_2X_2]Y$ (DP = *o*-phenylenebis(dimethylphosphine); $X^- = Cl^-, Br^-$; $Y^- = ClO_4^-, PF_6^-$) doped in the corresponding Co(III) lattices are reported. Principal values of *g* and the ligand superhyperfine tensors obtained are $g_{xx} = 2.1123$, $g_{yy} = 2.1157$, $g_{zz} = 2.0089$; for ^{35}Cl, $A_{xx} = 18.3 \pm 1$ G, $A_{yy} = 15.3 \pm 1$ G, $A_{zz} = 17.6 \pm 1$ G and for ^{31}P, $A\sigma = 13 \pm 1$ G, $A\pi = 5 \pm 1$ G, $A_{zz} = 43.6 \pm 1$ G, when $X^- = Cl^-$ and $Y^- = ClO_4^-$. For $X^- = Br^-$ and $Y^- = PF_6^-$, the values are $g_{xx} = 2.0961$, $g_{yy} = 2.1413$, $g_{zz} = 1.9936$; for ^{81}Br, $A_{xx} = 61 \pm 1$ G, $A_{yy} = 26 \pm 1$ G, $A_{zz} = 169 \pm 1$ G and for ^{31}P, *A* has a nearly isotropic value of 20 ± 2 G. Comparison is drawn to the previously studied DAS (*o*-phenylenebis(dimethylarsine)) analogue as well as among themselves.

Introduction

Ni(III) d^7 EPR has been the subject of many investigations reported hitherto in the literature.[2-13] Since the Ni nucleus is indifferent to EPR (natural abundance of even isotopes of Ni being 98.8%), studies on its complexes with group 6 donors have proved to be of only limited information due to lack of hyperfine interaction. But complexes of group 5B donors with almost 100% natural abundance of magnetic isotopes offer a wealth of data that is of considerable importance in the establishment of their electronic structures. The most illustrative case mentionable as a precursor to the present studies is that of the di(tertiary arsine) complex studied by Gray et al.[4] and Manoharan and Rogers.[3] EPR studies on these dihalo complexes reveal a highly delocalized molecular wave function for the unpaired electron as evidenced by the very well resolved superhyperfine structure from all the immediately bonded nuclei of the ligands. Bennett et al.[14] recently reported the synthesis and optical properties of a series of complexes of Ni(III) with DP and we thought it would be interesting to carry out EPR investigations on two of the complexes, namely, $[Ni(DP)_2Cl_2]ClO_4$ and $[Ni(DP)_2Br_2]PF_6$, to understand the nature of bonding from the analysis of superhyperfine coupling to the ligands. Fortunately, diamagnetic host lattices suitable for substitutional incorporation of these were also available.[14]

We describe the EPR of $[Ni(DP)_2Cl_2]ClO_4$ and $[Ni(DP)_2Br_2]PF_6$ in single crystals of the corresponding Co(III) analogues. Preliminary crystal structure data are available only for $[Co(DP)_2Cl_2]ClO_4$,[15] although no morphological details are known. Since there is no a priori requirement to know the molecular dispositions in the lattice for the derivation of principal values of the magnetic tensors,[16] we have gone ahead with single-crystal EPR studies on these systems. From the known geometries of the host lattice environment of the Co(III) ion and from the previous experience of the orientation of magnetic tensors relative to the molecular framework in the case of Ni(DAS),[4] we could obtain all the necessary information to understand the structure and bonding in these complexes. When complete X-ray data and morphological details become available, these results can be easily corroborated with respect to relation between magnetic axes and molecular framework. Powder EPR data have been used judiciously in unequivocally ascertaining the principal values of the magnetic tensors from crystal data. A simple LCAOMO approach has been used in the derivation of bonding parameters.

Experimental Section

$[Ni(DP)_2X_2]Y$ and the Co(III) analogues were prepared according to literature methods.[14] Single crystals for EPR measurements were prepared by slow evaporation of an acetonitrile solution of the Co(III) complex containing 2–3% of the Ni(III) salt. Powder samples were prepared similarly by grinding the microcrystals obtained as above. Solution measurements were made in a 1:1 mixture of acetonitrile and absolute alcohol.

All EPR spectra were measured on a Varian E-4 X-band spectrometer with a 100-kHz modulation. Field calibrations were made by using DPPH. All measurements were made at room temperature unless specified otherwise.

Results and Discussion

1. $Ni^{III}/[Co^{III}(DP)_2Cl_2]ClO_4$. The EPR spectrum of magnetically dilute polycrystalline $[Ni(DP)_2Cl_2]ClO_4$ shown in Figure 1 reveals an orthorhombic **g** tensor with the high-field *g* component containing 17 large intensity lines spaced with a set of smaller intensity lines. (The lowest field lines of this component overlap with the high-field lines of the low-field

0020-1669/79/1318-2520$01.00/0

Table I. g and A (Superhyperfine) Tensors for $(NiL_2X_2)^+$

	doped powder		doped crystal		
property	$[Ni(DP)_2Cl_2]^+$ X = ^{35}Cl, L = ^{31}P	$[Ni(DP)_2Br_2]^+$ X = ^{81}Br, L = ^{31}P	$[Ni(DP)_2Cl_2]^+$ X = ^{35}Cl, L = ^{31}P	$[Ni(DP)_2Br_2]^+$ X = ^{81}Br, L = ^{31}P	$[Ni(DAS)_2Cl_2]^+$ [b] X = ^{35}Cl, L = ^{75}As
g_{zz}	2.0092	1.9965	2.0089	1.9936	2.008 ($g_\parallel$)
g_{yy}	2.1106	2.1375 (est)	2.1157	2.1413	
g_{xx}		2.0686 (est)	2.1123	2.0961	2.142 ($g_\perp$)
A_{zz}(X)	−17.3	−170.8	−17.6 ± 1	−169 ± 0.1	−29
A_{yy}(X)			−18.3 ± 1	−61.7 ± 1	−50
A_{xx}(X)			−15.3 ± 1	−27 ± 1	−32
A_{zz}(L)	−43.3	−19.4	−43.6 ± 1	−19.4 ± 0.1	−32
$A\sigma$(L)		20 ± 2	−13 ± 1	20 ± 2	−8.5
$A\pi$(L)		20 ± 2	−5 ± 1	20 ± 2	−6.1
g_{av}			2.0789	2.0770	2.0973
g_{iso}			2.0881	2.0701	2.103[c]
A_{av}(X)			−17.1 ± 1	−86 ± 1	−37
A_{av}(L)			−20.5 ± 1	−19.8 ± 1	−15.8
A_{iso}(X)[a]			17.5 ^{35}Cl	83 ^{81}Br	17.0[c]
			14.5 ^{37}Cl	77 ^{79}Br	
A_{iso}(L)[a]			20.5	22	24.0[c]

[a] Values derived from the computer simulation of isotropic spectra, line width = 12 G for X = Cl^- and 22 G for X = Br^-. [b] Reference 4. [c] Reference 3.

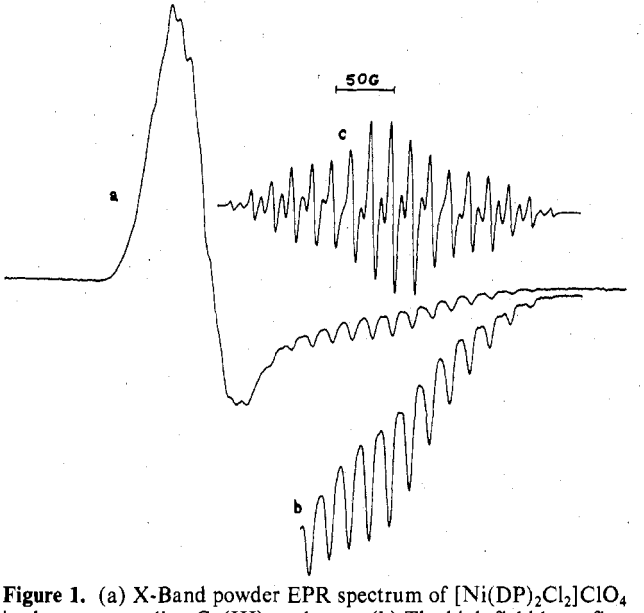

Figure 1. (a) X-Band powder EPR spectrum of $[Ni(DP)_2Cl_2]ClO_4$ in the corresponding Co(III) analogue. (b) The high-field hyperfine features at increased spectrometer gain. (c) The juxtaposition of the single-crystal spectrum with **B** parallel to the Cl–Ni–Cl direction.

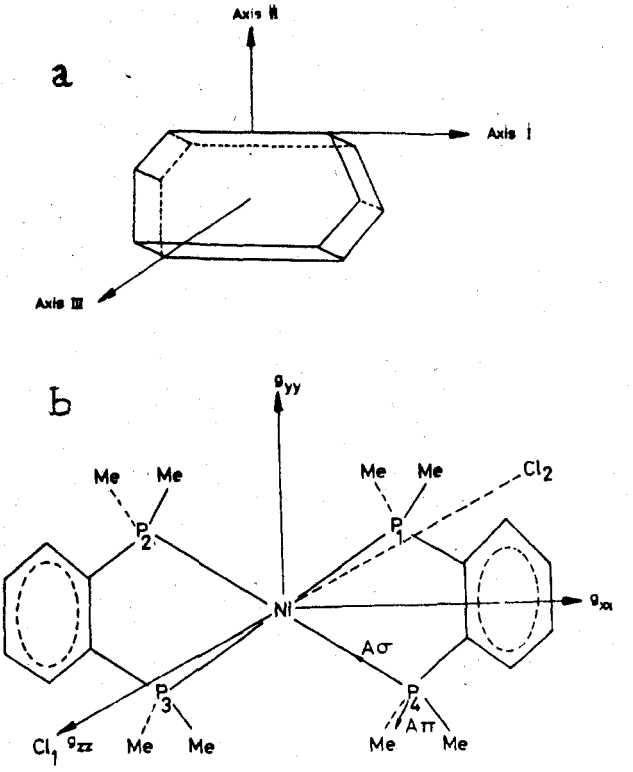

Figure 2. (a) External morphology of $[Co(DP)_2Cl_2]ClO_4$ crystal and the axes I, II, and III chosen for crystal EPR measurements. (b) The molecular framework of $[Ni(DP)_2Cl_2]^+$ showing the principal directions of the **g** tensor (which coincide with the **A** tensor of chlorine) and the **A** tensor of phosphorus.

g component.) This arises from a quintet hyperfine feature from four equivalent ^{31}P nuclei being further split by ^{35}Cl and ^{37}Cl such that $A(^{31}P) \approx 2.5A(^{35}Cl)$. The isotopic distribution of ^{35}Cl–^{37}Cl with their natural abundances also is evident in this. The **g** and **A** tensor values derived from the spectrum are given in Table I. Due to the near "axial symmetry" of the **g** tensor, g_{xx} and g_{yy} could not be estimated from this spectrum.

Single crystals used for the study have a morphology as shown in Figure 2a. It was possible, by careful alignment, to see that the three mutually orthogonal axes shown in Figure 2a coincide with the principal directions of the **g** tensor. Angular variation studies in these three orientations prove that all the sites in the unit cell are magnetically equivalent. It should be noted at this juncture that the host $[Co(DP)_2Cl_2]ClO_4$ has two crystal forms—tetragonal and triclinic. Crystallographic data on these two forms supplied by Robertson[15] proved to be of great use, enabling us to unravel the two different types of spectra obtained from crystals of different morphologies. Analysis of the direction cosines for the Cl–Co–Cl directions in the tetragonal unit cell (Z = 4) indicates two closely related sites with their unique axes making ±1.5° with one of the crystallographic axes. When we made a complete set of measurements on the tetragonal modification, the analysis was highly hampered by the presence of two inequivalent sites. However, the triclinic system (Z = 4 again) has only one magnetically distinct site[15] and hence the system (the one reported here) behaves extremely well, with the spectra maintaining a high degree of symmetry. But the magnetic parameters are the same for these two modifications.

By rotating the single crystal about axes parallel and perpendicular to the external edges, we found it possible to get a unique orientation, namely, axis I given in Figure 2a parallel to **B**, when the EPR spectrum obtained was exactly

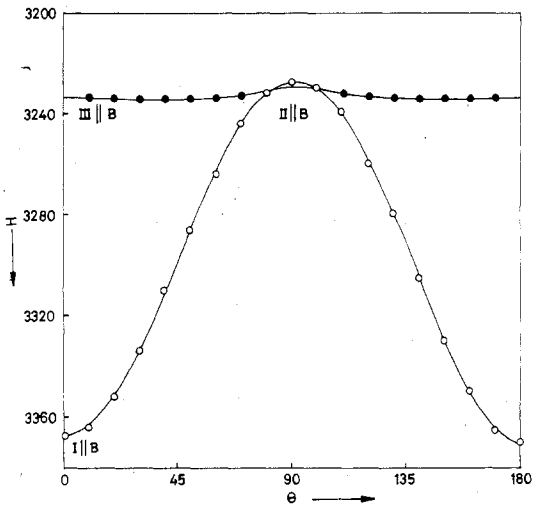

Figure 3. Angular variation of the center of gravity of spectra (corresponding to g (θ)) for rotation of the $Ni^{III}/[Co(DP)_2Cl_2]ClO_4$ single crystal about axes I and II of Figure 2.

identical with the high-field spectral group from the powder pattern. Figure 1c shows the juxtaposition of the EPR spectrum at such an orientation for comparison with the high-field features of the powder. It is at once evident that the morphological axis I corresponds to the axis Z, i.e., the Cl–Ni–Cl direction of the molecular framework shown in Figure 2b. This orientation corresponds to the maximum spread and hence is a principal direction of the magnetic tensors. By aligning the axis of rotation to coincide with the Cl–Ni–Cl direction, we now find it possible to get the other two principal values of the magnetic tensors by simply locating the major and the minor axes of the tensor ellipses. The angular variation of the g factors in the II–III plane and I–III plane which fortuitously coincide with the XZ and YZ (or vice versa) planes of the molecular framework are shown in Figure 3. In analogy with the nomenclature adopted for Ni(DAS)[4] axes I, II, and III correspond to the principal Z, Y, and X axes of the molecular frame. It was evident from the angular variation of the g and hyperfine features that the ^{35}Cl hyperfine tensor and **g** tensor are coincident. Representative spectra for **B** parallel to g_{xx} and g_{yy} are shown in Figure 4. However, for comparative understanding of the DAS and DP systems, we thought it advantageous to resolve the principal values of the phosphorus superhyperfine tensor in the XY plane along and perpendicular to the Ni–P bond, namely, $A\sigma$ and $A\pi$. These were measured by orienting the magnetic field in the principal "$g_{xx} - g_{yy}$" plane in such a way that **B** makes an angle 0 and 90° to a general P–Ni–P direction. With $B \| Z$ (axis I) we get g_{zz}, $A_{zz}(^{31}P)$, and $A_{zz}(^{35}Cl)$. Along axes II and III we derive g_{xx}, g_{yy}, and $A_{xx}(^{35}Cl)$ and $A_{yy}(^{35}Cl)$, respectively. It is to be noted that along the Ni–P bond phosphorus coupling is comparable to that of chlorine whereas perpendicular to this phosphorus coupling is, interestingly, one-third that of chlorine.

In order to decipher the electronic structure it becomes necessary to know the signs, at least relative signs, of the various hyperfine components. A knowledge of the isotropic coupling constants will definitely help in assessing the signs of the anisotropic hyperfine components. A well-resolved isotropic spectrum of this compound and the computer-simulated spectrum using a line width of 12 G are shown in Figure 5. The g_{av} obtained from single-crystal measurements agrees with the g_{iso} derived from the solution spectrum (see Table I).

Assuming direct spin transfer into the orbitals of the axial chlorine atoms and the in-plane σ and π orbitals of phosphorus atoms, we find it obvious that the A_{zz} of ^{35}Cl and ^{31}P must be of opposite signs, the former being positive.

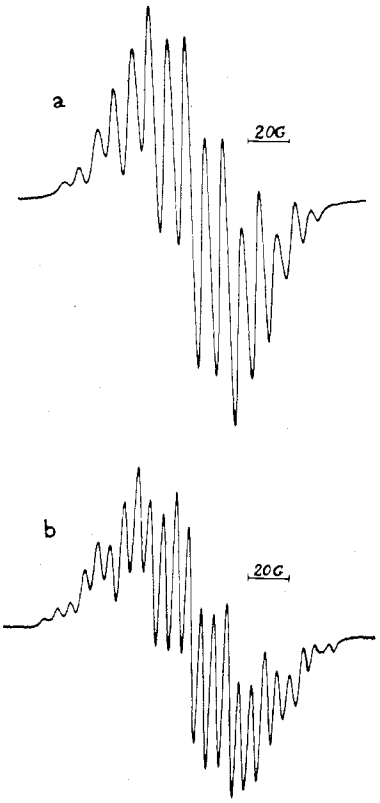

Figure 4. Typical EPR spectrum of $Ni^{III}/[Co(DP)_2Cl_2]ClO_4$ single crystal for (a) $\mathbf{B} \| g_{yy}$ and (b) $\mathbf{B} \| g_{xx}$. In both cases the four phosphorus hfc constants are equal. In (a) ^{31}P coupling is comparable to that of ^{35}Cl and in (b) $A(P) = {}^1/_3A(Cl)$.

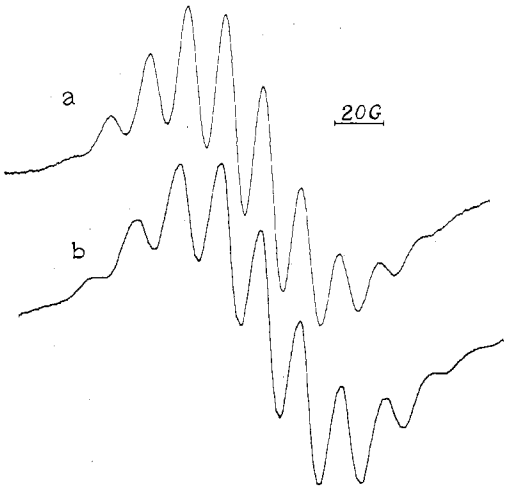

Figure 5. (a) Isotropic EPR spectrum of $[Ni(DP)_2Cl_2]ClO_4$ and (b) the corresponding computer-simulated spectrum.

Comparison with the isotropic ^{35}Cl and ^{31}P hyperfine coupling constants leads to all the principal hyperfine coupling constants being of the same sign. Molecular orbital calculations based on the spin distribution (vide infra) give results which are logical only when all ^{35}Cl and ^{31}P hyperfine coupling constants are negative. The values thus assigned for isotropic and anisotropic hyperfine coupling found in Table II can be used to calculate the spin densities on the ligand nuclei and hence the molecular wave function containing the unpaired electron. The isotropic and dipolar coupling constants for one unpaired electron in the appropriate orbitals were taken from ref 17. The experimental spin densities are also given in Table II.

Table II. Superhyperfine Tensors and Spin Densities

	$[Ni(DP)_2Cl_2]^+$ L = ^{31}P, X = ^{35}Cl		$[Ni(DP)_2Br_2]^+$ L = ^{31}P, X = ^{81}Br		$[Ni(DAS)_2Cl_2]^+$ [c] L = ^{75}As, X = ^{35}Cl	
	A, G	ρ, %	*A*, G	ρ, %	*A*, G	ρ, %
			L			
A_{iso}, ρ_{ns}	−20.5	0.6	−20	0.6	−15.8	0.5
$A_{dip.major}$, ρ_{np}	−25.4	12.3	*a*	4.9[b]	−16.7	9.1
$A_{dip.minor}$, ρ_{np}	−5.2	2.5	*a*	4.9[b]	−1	0.5
ρ_L		61.6		41.6		40.4
			X			
A_{iso}, ρ_{ns}	−17	1	−86	1	−37	2.2
$A_{dip.major}$, ρ_{np}	+2.0	2	−96	17	−14	14
$A_{dip.minor}$, ρ_{np}	+0.5	0.5	−24	4.25	−2	2
ρ_X		7		44.5		36.4
total $\rho_{L_4X_2}$		68.6		86.1		76.8

[a] Experimentally dipolar coupling constants could not be derived. [b] Estimated in comparison with the chloro compound (see text). [c] Using the hyperfine data in ref 4.

Table III. Overlap Integrals and Molecular Orbital Coefficients

	$[Ni(DP)_2Cl_2]^+$ L = P, X = Cl		$[Ni(DP)_2Br_2]^+$ L = P, X = Br		$[Ni(DAS)_2Cl_2]^+$ [b] L = As, X = Cl	
	$Sd_{z^2-\varphi_i}$	a_i[a]	$Sd_{z^2-\varphi_i}$	a_i[a]	$Sd_{z^2-\varphi_i}$	a_i[a]
$\varphi_{p_z}(X)$	0.074 24	0.141 42	0.067 13	0.412 3	0.074 24	0.374 16
$\varphi_s(L)$	0.103 01	0.077 46	0.103 01	0.077 46	0.095 24	0.067 82
$\varphi_{p\sigma}(L)$	0.137 80	0.350 7	0.137 80	0.022 73	0.128 83	0.301 66
$\varphi_{p\pi}(L)$	0	0.158 1	0	0.022 73	0	0.070 71
$\varphi_s(X)$	0.048 24	0.1	0.040 66	0.1	0.048 24	0.141 42
$\varphi_{p_x}(X)$	0	0.070 7	0	0.207 4	0	0.148 32
d_{z^2}		0.831 77		0.753 16		0.770 3

[a] Refer to eq 1. [b] Using the hyperfine data in ref 4.

Ground State of $[Ni(DP)_2Cl_2]^+$. Though the correct molecular symmetry could be only C_s or C_i in the crystal lattice, the NiP_4Cl_2 chromophore may be assigned a D_{2h} symmetry. The only optical transition observed at 14 771 cm^{-1} [14] for this complex can be assigned to $^2A_g \rightarrow {}^2B_{2g}$ and $^2A_g \rightarrow {}^2B_{3g}$ which are nearly degenerate. Following the comparison drawn between the d^7, $(t_2)^6e$ with one electron in the e shell and d^9, $(t_2)^6e^3$ with one hole in the e shell for $s = {}^1/_2$ systems,[18] we expect the *g* values to be near free spin with the deviations attributable to spin–orbit coupling. Evaluating the *g* values to first order by using the relation $g_\perp = 2.0023 - 6\lambda/\Delta$ ($\lambda = -272$ cm^{-1} for Ni(III)), we find $g_\perp$ turns out to be 2.110 48 (observed values are $g_{xx} = 2.1123$ and $g_{yy} = 2.1157$) and $g_\parallel$ is found to be near free spin. Though this excludes contribution from ligand spin–orbit coupling, a simple correlation of this kind indicates a d_{z^2} ground state for this ion with the d-level ordering, $a_g(x^2-y^2) < b_{2g}(xz) < b_{3g}(yz) < a_g(z^2) < b_{1g}(xy)$. The LCAO–MO for the unpaired electron can be written as[4] shown in eq 1, where a_1 and a_2, a_3, etc. are metal and ligand

$$a_g(d_{z^2}) = a_1 d_{z^2} + a_2\varphi_{p_z}(Cl) + a_3\varphi_s(P) - a_4\varphi_{p\sigma}(P) - a_5\varphi_{p\pi}(P) - a_6\varphi_s(Cl) - a_7\varphi_{p_x}(Cl) \quad (1)$$

orbital coefficients, respectively, and the φ's are ligand orbital combinations defined in eq 2.

$$\varphi_{p_z}(Cl) = 2^{-1/2}[p_z(Cl_1) - p_z(Cl_2)]$$
$$\varphi_s(P) = (1/2)[s(P_1) + s(P_2) + s(P_3) + s(P_4)]$$
$$\varphi_{p\sigma}(P) = (1/2)[p_x(P_1) - p_x(P_2) - p_x(P_3) + p_x(P_4)]$$
$$\varphi_{p\pi}(P) = (1/2)[p_y(P_1) + p_y(P_2) - p_y(P_3) - p_y(P_4)]$$
$$\varphi_s(Cl) = 2^{-1/2}[s(Cl_1) + s(Cl_2)]$$
$$\varphi_{p_x}(Cl) = 2^{-1/2}[p_x(Cl_1) - p_x(Cl_2)] \quad (2)$$

The ligand orbital coefficients are directly obtained from the spin-density data (Table III). Imposing the normalization condition on eq 1 we get eq 3, where S_{ij}'s are the overlap

$$a_1^2 + 2a_1\sum_{i\neq j}^{7} a_i S_{ij} = 1 \quad (3)$$

integrals in Table III, evaluated by using Richardson's functions[19] for the metal atom and Clementi's functions[20] for the ligands. Using eq 3 and the a_i's, we obtained the metal orbital coefficient a_1. Comparison of these coefficients with those for the dichloro complex of Ni(DAS) gives an idea of the quantitative changes in the modes of bonding as we go from P to As in group 5B.

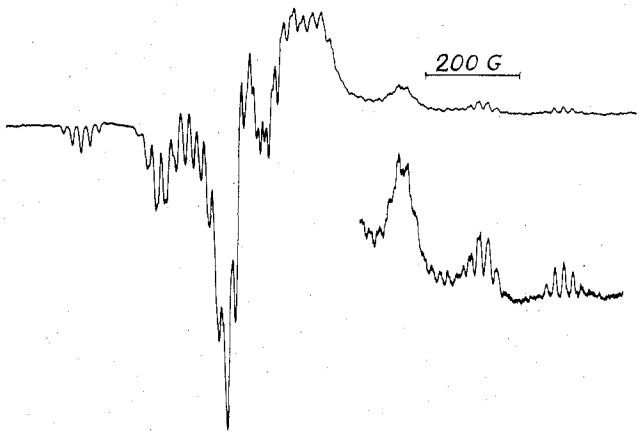

Figure 6. Powder EPR spectrum of $Ni^{III}/[Co(DP)_2Br_2]PF_6$. The inset shows the high-field features at increased gain.

2. $Ni^{III}/[Co(DP)_2Br_2]PF_6$. The analogous bromo complex was also studied on exactly similar lines as above. The doped powder spectrum was poorly resolved at room temperature. But, around −50 °C all the features are very well resolved as shown in Figure 6. The high-field *g* feature corresponding

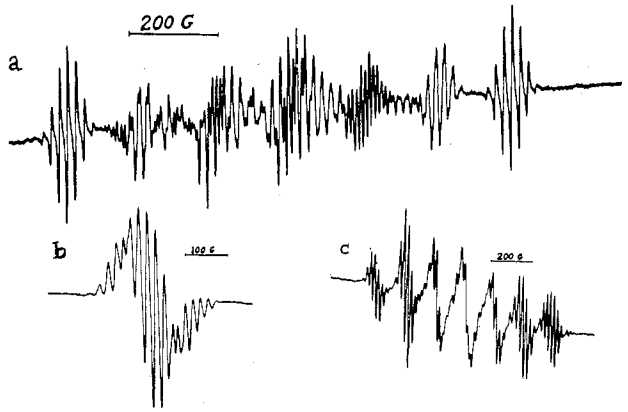

Figure 7. (a) Single-crystal EPR spectrum of $Ni^{III}/[Co(DP)_2Br_2]PF_6$ with one of the magnetically distinct sites having its Br–Ni–Br direction parallel to the magnetic field. (b) EPR spectrum of $Ni^{III}/[Co(DP)_2Br_2]PF_6$ single crystal when the magnetic field is parallel to the g_{yy} direction of Figure 2. (c) Typical spectrum of $Ni^{III}/[Co(DP)_2Br_2]PF_6$ single crystal for **B** in the I–II plane. The two sites are equivalent in this plane.

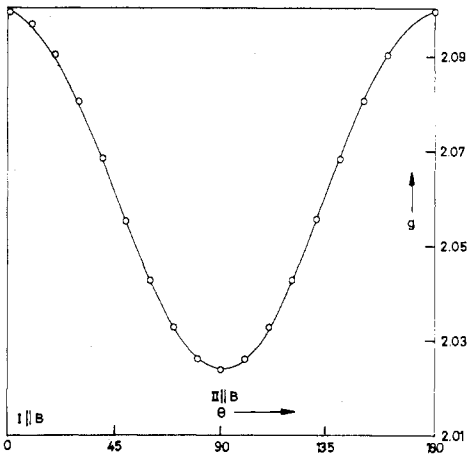

Figure 8. Angular variation of the **g** tensors for rotation of the crystal about axis III. The two sites are equivalent in this plane.

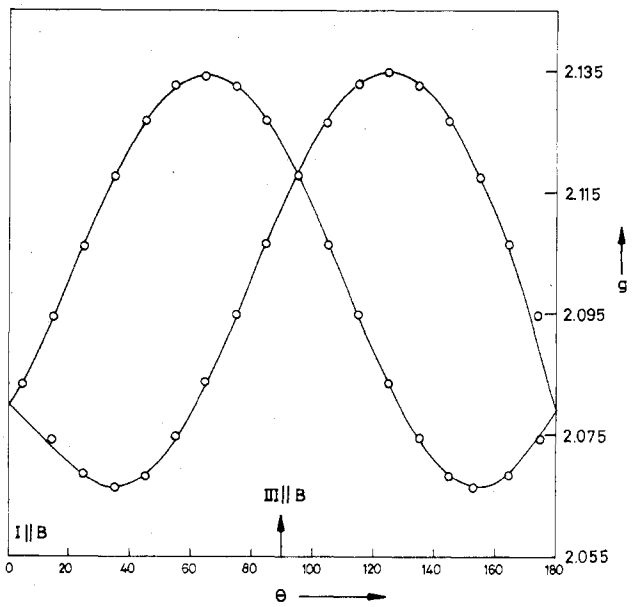

Figure 9. Angular variation of the *g* factors for the two magnetically distinct sites for rotation about axis II.

to maximum bromine hyperfine coupling masks the hyperfine structure corresponding to the other two *g* features. The spectrum is complicated because of the bromine isotope effects. The statistical probability of bromine pairs occurring as ^{81}Br–^{81}Br, ^{79}Br–^{81}Br, and ^{79}Br–^{79}Br based on the natural abundances turns out to be 1:2:1. This results in an artifact of giving a septet feature at the extremes of the spectra and more complicated hyperfine features elsewhere. The **g** and **A** tensor components derived from this spectrum are listed in Table I. From the powder data, only g_{zz}, Br(A_{zz}), and P(A_{zz}) could be exactly evaluated. (These compare very well with the single-crystal data.) Only rough estimates of the *xx* and *yy* components of *g*, Br(*A*), and P(*A*) could be obtained and hence they are derived only from single-crystal data. Second-order corrections due to large Br hyperfine coupling constants have been made in deriving the magnetic parameters.

Single-crystal studies on this system are fraught with additional complications arising out of two magnetically distinct sites. Lack of crystal structure information at present on the Co(III) host lattice leaves their exact dispositions in the unit cell uncertain. However, angular variation studies in three mutually orthogonal orientations give all the required information. The morphology of this crystal and the three axes chosen for rotation also correspond to those given in Figure 2a. Here again, it was possible to identify g_{zz} which coincides with A_{zz} of bromine and those of the four phosphorus nuclei in the plane, by comparison with the powder spectrum. Figure 7a shows the most representative spectrum in orientation I (**B** parallel to axis I which is identical with $\mathbf{B}\|g_{zz}$ for one of the sites). Since the Br hyperfine coupling constant is largest here, the isotope separation is a maximum and nearly equal to the ^{31}P hyperfine coupling constant (cf. discussion on the powder spectrum). This accounts for the extreme set of hyperfine features of a septet with the intensity distribution 1:6:15:20:15:6:1.

When we examine the inner sets, the bromine isotopic separations will be smaller giving rise to a maximum of 15 lines (3 × 5) on the inner Br hyperfine features. Added to this is the complication due to the presence of two magnetically distinct sites. Additional lines due to "forbidden transitions" and variations from the expected intensity ratios from simple considerations due to the large quadrupole moment of the bromine nuclei are also responsible for the highly complex spectra. These aspects are under further investigation and will be reported later.

In orientation II (**B** perpendicular to the Br–Ni–Br direction), we have the most compressed spectrum (Figure 7b). The simplicity of the spectrum and the nearly equal spacings of the lines suggest that, in this orientation, the field vector is along one of the principal directions, namely, g_{yy}, which bisects the P–Ni–P angle, reinforcing the correctness of the identification of the principal *Z* direction with axis I. Rotation about axis II reveals the two sites moving out of phase with each other. The bromine hyperfine coupling constant is comparable to that of ^{31}P, the latter remaining nearly isotropic in all orientations in this plane. In orientation III, there is a near coincidence of both the sites throughout the rotation. Figure 7c shows the spectrum illustrative of this and Figure 8 indicates the *g*-factor variation for rotation of the field vector in this orientation.

Figure 9 shows the angular variation of the *g* factors in I–III plane. The diagonalized **g**-tensor values and superhyperfine tensor components[16] are in Table I. The isotropic *A* values obtained from the computer simulation of the experimental solution spectrum shown in Figure 10 not only supports the magnitude of the various hyperfine tensor values for this ion but gives a clue to their relative signs, which are similar to the chloro analogue discussed above. The spin densities and bonding parameters derived as in the case of the dichloro complex can be found in Tables II and III. Here, the accuracy

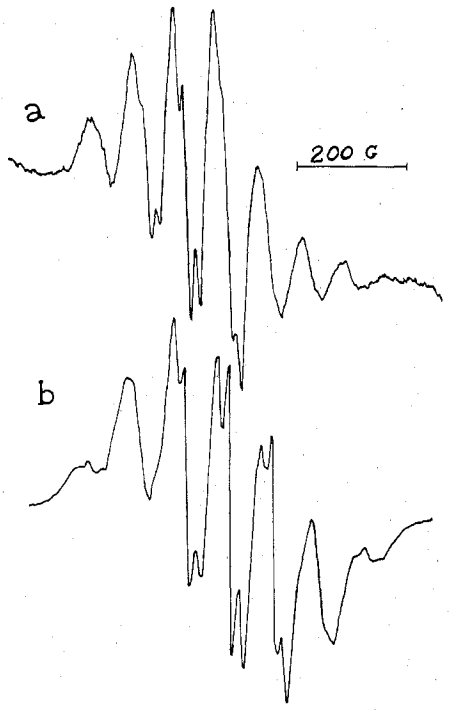

Figure 10. (a) Isotropic spectrum of $[Ni(DP)_2Br_2]PF_6$ along with (b) the computer -simulated spectrum.

is limited by the probable error in the ^{31}P superhyperfine tensor values. The observed isotropicity of the phosphorus superhyperfine tensor can only be belying the actual dipolar densities because it is not reasonable to expect that the phosphorus π bonding becomes negligible in going from the dichloro to the dibromo complex. This apparent isotropicity is definitely an artifact of almost equal spin-density distribution in the three p orbitals of phosphorus, namely, the in-plane π, σ, and the out-of-plane π orbitals. The in-plane p orbitals of σ and π symmetry transform as the a_g representation and hence directly partake of the unpaired density via overlap. However, in view of the nearly 45% of spin density on the bromine ligand, there must be considerable back-bonding via Br p_x and p_y orbitals and, presumably, the d orbitals of Br to the phosphorus out-of-plane, p_z orbitals. Such a "back-bonding" will be quite feasible since the actual symmetry of the complex is only C_i. Hence, we have assumed that the spin densities on phosphorus of these chloro and bromo complexes are almost identical except that in the latter there is an equal distribution of the dipolar spin density in the three p orbitals.

The two complexes studied, together with the results of Gray et al.[4] on the DAS analogue, show that in the Ni(III) complexes with group 5B donor ligands there is considerable delocalization of the unpaired density. Ligand hyperfine tensors and an approximate LCAO–MO approach show that there is an increase of covalency in the order $[Ni(DP)_2Cl_2]^+ < [Ni(DAS)_2Cl_2]^+ < [Ni(DP)_2Br_2]^+$. However, in the bromo complex, there is considerable σ delocalization onto the axial bromines, leading to a net higher covalency. It is striking that the covalency increases whenever the 4s and 4p orbitals are involved. This is obviously due to the extended radial wave functions of 4s and 4p orbitals. The $[Ni(DP)_2Cl_2]^+$ is the least covalent in this series since both phosphorus and chlorine orbitals involved in the MO formation are of the 3s and 3p type, while in the other two complexes, either bromine or arsenic provides the extended 4s, 4p components resulting in a higher delocalization. This would indicate that the complex ion $[Ni(DAS)_2Br_2]^+$ will probably have almost the entire unpaired density on the ligands themselves.

Acknowledgment. We are thankful to Dr. G. B. Robertson for the X-ray data on $[Co(DP)_2Cl_2]ClO_4$ and to NCERT, New Delhi, for a fellowship to C.N.S.

Registry No. $[Ni(DP)_2Cl_2]ClO_4$, 60536-62-1; $[Ni(DP)_2Br_2]PF_6$, 70528-10-8.

References and Notes

(1) (a) Indian Institute of Technology. (b) The Australian National University.
(2) P. Kreisman, R. E. Marsh, J. Preer, and H. B. Gray, *J. Am. Chem. Soc.*, **90**, 1067 (1968).
(3) P. T. Manoharan and M. T. Rogers, *J. Chem. Phys.*, **53**, 1682 (1970).
(4) P. K. Bernstein and H. B. Gray, *Inorg. Chem.*, **11**, 3035 (1972).
(5) C. Corvaja and P. L. Nordio, *Ric. Sci.*, **38**, 44 (1868).
(6) A. H. Maki, N. Edelstein, A. Davison, and R. H. Holm, *J. Am. Chem. Soc.*, **86**, 4580 (1964).
(7) E. I. Steifel, J. H. Waters, E. Billig, and H. B. Gray, *J. Am. Chem. Soc.*, **87**, 3016 (1965).
(8) A. Davison, N. Edelstein, R. H. Holm, and A. H. Maki, *Inorg. Chem.*, **2**, 1227 (1963).
(9) A. H. Maki, T. E. Berry, A. Davison, R. H. Holm, and A. L. Balch, *J. Am. Chem. Soc.*, **88**, 1080 (1966).
(10) A. Davison, N. Edelstein, R. H. Holm, and A. H. Maki, *J. Am. Chem. Soc.*, **85**, 2029 (1963).
(11) J. W. Orton, P. Auzins, J. H. E. Griffiths, and P. E. Wertz, *Proc. Phys. Soc., London*, **78**, 554 (1961).
(12) W. Low and J. T. Suss, *Phys. Lett.*, **7**, 310 (1963).
(13) R. Lacroix, U. Hochli, and K. A. Müller, *Helv. Phys. Acta*, **37**, 627 (1964).
(14) L. F. Warren and M. A. Bennett, *Inorg. Chem.*, **15**, 3126 (1976).
(15) G. B. Robertson, private communication.
(16) D. S. Schonland, *Proc. Phys. Soc., London*, **73**, 788 (1959).
(17) P. W. Atkins and M. C. R. Symons, "The Structure of Inorganic Radicals", Elsevier, Amsterdam, 1967.
(18) A. Abragam and B. Bleaney, "Electron Paramagnetic Resonance of Transition Ions", Oxford, 1970.
(19) J. W. Richardson, W. C. Nieuport, R. R. Pavel, and W. F. Edgell, *J. Chem. Phys.*, **36**, 1057 (1962).
(20) E. Clementi, "Tables of Atomic Functions", I.B.M., 1965.